Available online at www.sciencedirect.com
ScienceDirect
Journal of Sound and Vibration 321 (2009) 1171–1185
JOURNAL OF SOUND AND VIBRATION
www.elsevier.com/locate/jsvi

Detecting the crankshaft torsional vibration of diesel engines for combustion related diagnosis

P. Charles[a], Jyoti K. Sinha[a,*], F. Gu[b], L. Lidstone[a], A.D. Ball[b]

[a]*School of Mechanical, Aerospace and Civil Engineering, The University of Manchester, P.O. Box 88, Manchester M60 1QD, UK*
[b]*School of Computing & Engineering, University of Huddersfield, Huddersfield, Queensgate HD1 3DH, UK*

Received 29 May 2008; received in revised form 19 September 2008; accepted 28 October 2008
Handling Editor: C.L. Morfey
Available online 19 December 2008

Abstract

Early fault detection and diagnosis for medium-speed diesel engines is important to ensure reliable operation throughout the course of their service. This work presents an investigation of the diesel engine combustion related fault detection capability of crankshaft torsional vibration. The encoder signal, often used for shaft speed measurement, has been used to construct the instantaneous angular speed (IAS) waveform, which actually represents the signature of the torsional vibration. Earlier studies have shown that the IAS signal and its fast Fourier transform (FFT) analysis are effective for monitoring engines with less than eight cylinders. The applicability to medium-speed engines, however, is strongly contested due to the high number of cylinders and large moment of inertia. Therefore the effectiveness of the FFT-based approach has further been enhanced by improving the signal processing to determine the IAS signal and subsequently tested on a 16-cylinder engine. In addition, a novel method of presentation, based on the polar coordinate system of the IAS signal, has also been introduced; to improve the discrimination features of the faults compared to the FFT-based approach of the IAS signal. The paper discusses two typical experimental studies on 16- and 20-cylinder engines, with and without faults, and the diagnosis results by the proposed polar presentation method. The results were also compared with the earlier FFT-based method of the IAS signal.

1. Introduction

Early fault detection and diagnosis for medium-speed diesel engines is important to ensure reliable operation throughout the course of their service. This type of engine is used for ship propulsion and is the primary driver in many industrial applications such as large compressors, ferries and large electrical generators as well as many large on and off road vehicles. Many speed-based condition-monitoring techniques have been developed and proposed for rotating and reciprocating machines and engines. Gu et al. [1] investigated the instantaneous angular speed (IAS) signal characteristics to detect and diagnose faults of piston engines. Feldman and Seibold [2] detected the size and location of damage in a rotor bar system using IAS or torsional vibration. Sweeney and Randall [3] demonstrated that a gear-based power transmission system has speed

*Corresponding author. Tel.: +44 (0) 161 306 4639.
E-mail address: jyoti.sinha@manchester.ac.uk (J.K. Sinha).

0022-460X/$ - see front matter © 2008 Elsevier Ltd. All rights reserved.
doi:10.1016/j.jsv.2008.10.024

fluctuations. Yang et al. [4] presented a dynamic model for simulating the IAS and its waveforms of a diesel engine. The simulated results have been validated by experimental data and the characteristic parameters for detecting the faults relating to the gas pressure in the cylinder are obtained successfully. Numerous researchers, such as Mauer [5,6], Rizzoni [7] and Margaronis [8] have also paid attention to this issue.

Almost all of these techniques were developed on small engines and their performance varies largely between applications. This research presents an investigation into the detection capability of using the encoder signal from a magnetic pickup unit (MPU) of medium-speed diesel engines to investigate the IAS signal from the engine's flywheel.

The main advantages of the IAS measurement technique are:

- Less noise contamination.
- It is directly related to machine dynamics.
- An inexpensive encoder.
- It is easy to install.
- No periodic calibration is needed.
- The results are easy to interpret and therefore a more accurate diagnosis is possible.

For the measurement of angular speed many methods have attempted to improve measurement performance using a different strategy to process encoder signals. The possible phase-demodulation techniques can be classified into time-interval and fast Fourier transform (FFT)-based techniques. In the time-interval technique the intervals between pulses have to be measured because they are inversely proportional to the variation of the speed. The calculation of the pulse interval is based on the measurement of the zero-crossing points between successive pulses of the encoder signal. In this research the time-interval method is implemented to compare with the FFT-based approach.

In the first phase of the study, an improved signal processing algorithm has been developed to construct the IAS signal from the raw data for the speed measurement using the magnetic encoder signal. The earlier FFT-based technique was then applied to the improved IAS signals (the crankshaft torsional vibration) and tested on the two typical experimental diesel engines with and without a combustion fault. The FFT analysis of the IAS signals shows potential for identifying the faulty engine, but the identification process is subjective and needs to be compared to data from the engine without fault. Hence an alternate method has been developed here, which again uses the IAS signals, but processes and presents the data in a novel way i.e. using the polar coordinate system. The four-stroke engines used complete one cycle of firing within two revolutions of the crankshaft. The required 720° duration of the engine cycle is represented by the 360° polar presentation system, where the radius of the system corresponds to the IAS amplitudes. The cylinder firing order (Table 1) of the engine is represented by an angle of the coordinate system in reference to each individual cylinder. The advantage of this approach is that it not only identifies the faulty engine but also pin points the faulty cylinder or cylinders.

This paper is organised into five sections. Section 2 explains the improved method for the estimation of the IAS signal and the novel polar presentation method to aid understanding. Section 3 discusses the general test rig facilities and the engine specifications. Section 4 presents an experimental evaluation of a 16-cylinder medium-speed diesel engine; as well as a comparison of the results between the earlier FFT-based method and

Table 1
Engines specifications.

	16-cylinder	20-cylinder
Maximum power	8400 kW at 740 rev/min	9000 kW at 1000 rev/min
Engine type	Four-stroke vee form	Four-stroke vee form
Flywheel teeth	152	304
Firing order	A1-B3-A3-B7-A7-B5-A5-B8-A8-B6-A6-B2-A2-B4-A4-B1	A1-B3-A3-B6-A6-B9-A9-B7-A7-B10-A10-B8-A8-B5-A5-B2-A2-B4-A4-B1

the novel polar representation method, along with its key benefits. Section 4 also illustrates a diagnosis of a 20-cylinder diesel engine and signal distinctions by the novel polar method. This is a typical example where the firing angle of all 20 cylinders is not equally distributed. The final section reviews the advantages of the technique and explains the novelty of the method for condition monitoring of medium-speed diesel engines.

2. Torsional vibration-based signal processing method

Engines always have some degree of torsional vibration during operation due to their reciprocating nature. Whilst the crankshaft of an engine rotates, the piston goes through different engine strokes. The rotation of the crankshaft increases the cylinder pressure as the piston approaches top dead centre (TDC) on the compression stroke. Ignition and combustion increases the pressure just after TDC and the pressure starts to decrease when the piston moves down to bottom dead centre (BDC) and the combustion gases expand. The pressure on the piston generates the tangential force (via the connecting rod) that does useful work and increases the rotational speed of the crankshaft during this combustion stroke, whereas the compression stroke decreases the engine's angular velocity. The changing rotational speed results in the speed fluctuations of the crankshaft, with the main speed change expected during the combustion stroke of the firing cylinder. Taking into account, the number of cylinders firing during one turn of the crankshaft, the main difficulty is detecting the combustion stroke of the firing cylinders within one engine cycle. However, this speed fluctuation, in terms of the IAS signal (which represents the crankshaft torsional vibration), has been used for such identification based on the assumption that any fault in a cylinder, small or large, would affect the torsional vibration predominantly [9].

Extraction of IAS from an encoder pulse signal is a critical procedure for speed-based condition monitoring. The obvious means of achieving this is to measure the crankshaft angular rotation over a definite period of time. If the period of time over which the speed is calculated is reduced, the average speed measured will be more representative of any speed fluctuations. The estimation of the IAS signal, based on the frequency modulated (FM) signal and according to the signal processing techniques involved, can be categorised into four main groups: zero-cross, time-domain, frequency-domain and time–frequency methods. Vakman [10] showed that the frequency-domain-based method provides higher precision for instantaneous frequency estimation than the usual zero-cross and time-domain methods. The frequency-domain method is adopted in this paper for IAS estimation, because condition monitoring demands that the IAS estimation be as accurate as possible. However, an approach has been developed which relies on the parameters used for signal processing to determine the IAS. In this research the time-interval method is implemented only to provide comparison with the frequency-domain (FFT-approach) method.

The IAS data taken from the motion of the crankshaft is a typical FM signal. The signal for varying angular speed can be presented as [11]

$$\begin{aligned} s(t) &= A\cos\left[N\omega_0 t + N\int_0^t \delta\omega(t)\,\mathrm{d}t + \phi_c\right] \\ &= A\cos[\omega_c t + \phi(t)] \end{aligned} \tag{1}$$

where A is the amplitude of the signal, N the number of teeth on the flywheel, $\omega = \omega_0 + \delta\omega(t)$ the angular speed with the constant part ω_0 and the varying part $\delta\omega(t)$, ϕ_c the initial phase, $\omega_c = \omega_0 N$ the shaft encoder carrier frequency and $\phi(t) \cdot \delta\omega(t)$ the phase deviation and is referred to as the information signal [9].

To obtain the IAS from the signal described in Eq. (1), the frequency domain method firstly constructs an analytic Hilbert transformation (HT) representation of the signal and therefore the IAS is calculated by

$$w(t) = \frac{\mathrm{d}\phi_s}{\mathrm{d}t} = \frac{\mathrm{d}}{\mathrm{d}t}\mathrm{Im}\{\ln[w(t)]\} = \mathrm{Im}\left[\frac{\dot{w}(t)}{w(t)}\right] \tag{2}$$

where $\phi_s(t) = \omega N t + \phi_c$ is the instantaneous phase of the signal, $w(t)$ the IAS, $\dot{w}(t)$ the differentiation signal and $\mathrm{Im}[\dot{w}(t)/w(t)]$ is the imaginary part of $[\dot{w}(t)/w(t)]$.

Random noise always exists in the IAS signal. Firstly the mechanical components produce fluctuations and secondly the measurement process has uncertainties and thermal noise. Gu et al. [1] showed that the signal-to-noise ratio of a FM signal can be enhanced by using a toothed wheel with a high resolution.

The FFT-based technique using the HT can be summarised in the following steps:

- Apply a FFT to the real signal. Although the amplitude at the fundamental frequency is dominant, there is also a number of higher order harmonics caused by the rectangular nature of the waveform.
- Find the carrier frequency by calculating the amplitude spectrum based on the FFT result. A figure would also show the angular modulation by the spread of the sidebands around the carrier frequency.
- To achieve the real analytic representation, set the FFT results in the negative frequency range to zeros.
- Band-pass filter the signal by keeping the FFT results around the carrier frequency and setting the others in the positive frequency range to zeros to eliminate the distortion.
- Shift the filtered FFT block on the right side of the carrier frequency to the beginning of the positive frequency range and shift the filtered FFT block on the left side to the negative frequency range of the filtered window.
- The angle-varying signal can be calculated by performing the IFFT of the shifted spectrum (obtains the complex angle variation signal in the time-domain).
- Finally, differentiate the angular displacement to get the displacement variation or IAS signal. Remove the high-frequency noise of the signal by low-pass filtering. Care must be used in this stage as some high-frequency components may relate to real components in angle changes.

2.1. Novel polar presentation method

Although the IAS time waveform and its FFT spectrum seem to detect the combustion related faults in diesel engines, the identification process is subjective. Hence a novel representation method based on the polar coordinate system has been introduced. It is shown in Fig. 1. The polar plot is a two dimensional coordinate system in which each point in the graph is determined by an angle and a distance. Also called the radial

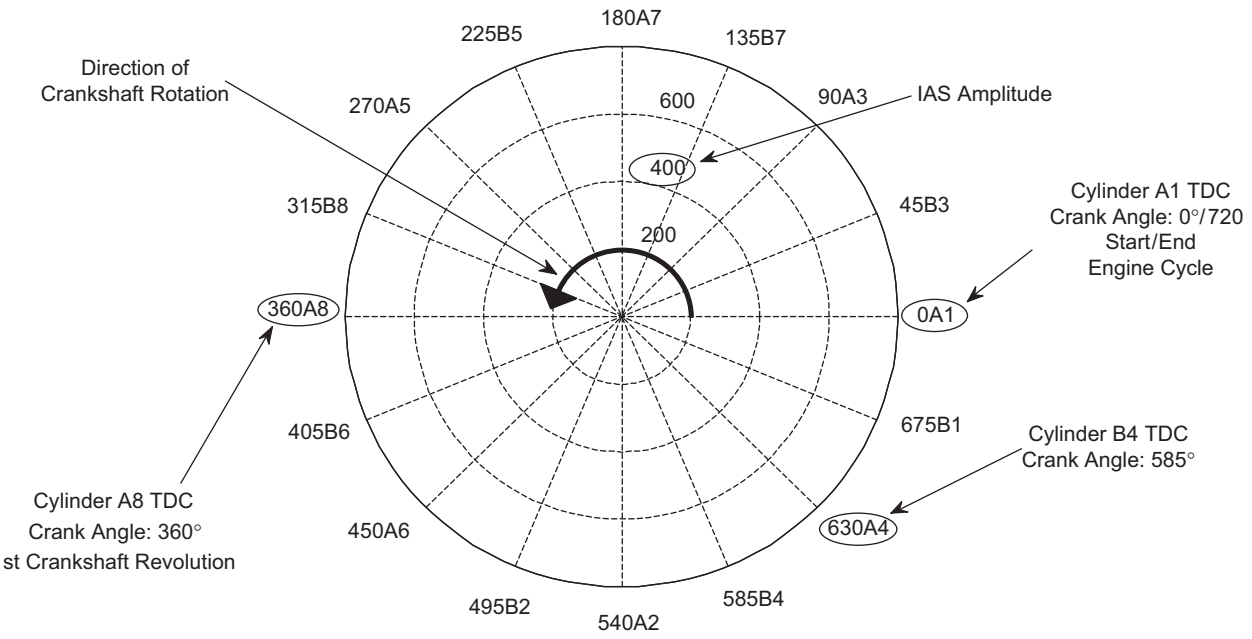

Fig. 1. Novel polar plot.

coordinate τ and angular coordinate ϕ. The Cartesian coordinates x and y can be converted to the polar coordinate τ by the Pythagorean theorem. To determine the angular coordinate ϕ, and for $\tau = 0$, ϕ can be set to any real value and for $\tau \neq 0$, ϕ must be limited to an interval of size 2π. The radius of the system corresponds to the IAS amplitude and the 360° angular coordinate is used to represent the 720° duration of the engine cycle. One engine cycle is equal to two revolutions of the crankshaft and if the engine has N_c cylinders, the number firing during one turn of the crankshaft N_f is calculated by

$$N_f = \frac{N_c}{2} \text{ (for a four-stroke engine)} \tag{3}$$

Assuming that the N_f firings are equally spaced in angle so the angle between consecutive firings of a four-stroke engine is given by

$$\phi_c = \frac{720^\circ}{N_c} \tag{4}$$

and the period of time between the consecutive cylinders firing is given by

$$T_f = \frac{T_{rev}}{N_f} = \frac{T_{cs}}{N_c} \tag{5}$$

where $T_{cs} = 2T_{rev}$ is the period of the engine's combustion stroke in seconds and therefore the firing frequency f_f is given by

$$f_f = \frac{1}{T_f} \tag{6}$$

Fig. 1 represents the polar presentation of a 16-cylinder engine (eight-cylinders in bank A and eight-cylinders in bank B) and the firing angle between two cylinders is a constant angle of 45° of the crank shaft rotation. The angle 0° represents the TDC position of the first cylinder A1, 45° the TDC position of cylinder B3 and 90° represents the cylinder A3 (according to the firing order) and so on. The amplitude of the torsional vibration (IAS) for each cylinder can be plotted as the radius of the polar plot. Hence the proposed presentation relates the amplitude of the vibration with respect to each cylinder and helps to identify the faulty cylinders in an engine. However, it should be noted that as the number of cylinders increases the firing angle between consecutive firings decreases. This simply means that the polar presentation of the IAS time waveform will struggle to identify the faulty cylinder or cylinders. Hence, to avoid such a situation and enhance the discriminating capability (between the faulty and healthy cylinders), the raw IAS time waveform has been divided into the following two categories (using the low-pass filter while plotting the suggested polar presentation plot for the diagnosis):

(1) *Low-frequency range* (up to $0.5f_f$) including frequencies up to the sub-harmonics of the firing frequency.
(2) *High-frequency range* (up to $2f_f$—twice the firing frequency) including the firing frequency component and its higher components.

The advantage of these two kinds of the IAS time waveform is that combustion related faults expected to be related to either the sub-harmonic or higher harmonics of the firing frequency can be clearly seen in the polar presentation plots and the faulty cylinder/cylinders can be identified which is essential for any diagnosis method. Typical experimental examples are discussed in Sections 4.2 and 4.3.

3. Test rig facilities

The 16- and 20-cylinder V-type engines have been used to evaluate the proposed method. The 16-cylinder engine has been tested at 0%, 25%, 50% and 75% load and an average speed of 750 rev/min for an engine under healthy conditions and at 25% and 75% for an engine with a misfiring cylinder. The angle ϕ_c between the consecutive cylinders firing was 45° crank angle and the firing frequency f_f was 100 Hz.

The 20-cylinder engine has been tested at 0% and 50% load and the average speed of 1000 rev/min. The angle ϕ_c between consecutive firings was not equally spaced for this case. Here the angle ϕ_c has two values, 20° and 52°, and the average firing frequency was 166 Hz as there were 10 cylinders firing during one turn of the crankshaft. Table 1 shows the engine maximum power output, engine type, amount of flywheel teeth and the firing order.

3.1. Data acquisition (DAQ) system

Two prototype DAQ systems were developed in this research. The DAQ system collects multiple channels of IAS data, acoustic data and vibration data and monitors faults from individual cylinders and mechanical systems. System A is a laptop controlled eight channel data logging system with a resolution of 16 bits and a maximum sampling rate of 100 kHz per channel. It is supplied with various anti-aliasing filters and an internal amplification of up to a gain of 1000. System B is equipped with 16 analogue channels, a resolution of 12 bits and a sampling frequency up to 2.2 MHz for high-speed IAS acquisition. These two systems have been linked together through an external trigger mechanism for time-synchronised DAQ.

3.2. Sensing method

The speed fluctuation of the crankshaft is detected by using a MPU mounted to the flywheel of the engine. The MPU produces a potential difference when a magnetic material passes through the magnetic field at the end of the sensor. In this way, the profile of the gear teeth on the flywheel, used by the starter motor, is detected by the MPU during engine operation. Assuming that the gear teeth are distributed uniformly, there is little noise interference and the speed of the engine is constant, the signal from the MPU is equal to a homogeneously periodic waveform. A variation of the signal's homogeneity is caused by a change of the angular acceleration and is detected instantaneously by the teeth passing the MPU. A reference signal from a tachosensor for the flywheel corresponding to the TDC mark shown in Fig. 2 is used to mark the reference cylinder firing for the data presentation.

To identify the firing of the first cylinder, on a four-stroke engine, either the vibration or the acoustics of the cylinder has to be recorded by placing a sensor on or close to the cylinder. With every revolution of the crankshaft the TDC sensor registers one peak. However, this crank position can be either the first cylinder firing or the sixth cylinder firing in the case of a 12-cylinder engine. Because the major amplitudes of the vibration output are localised around a particular angular position, e.g. when the combustion occurs in the

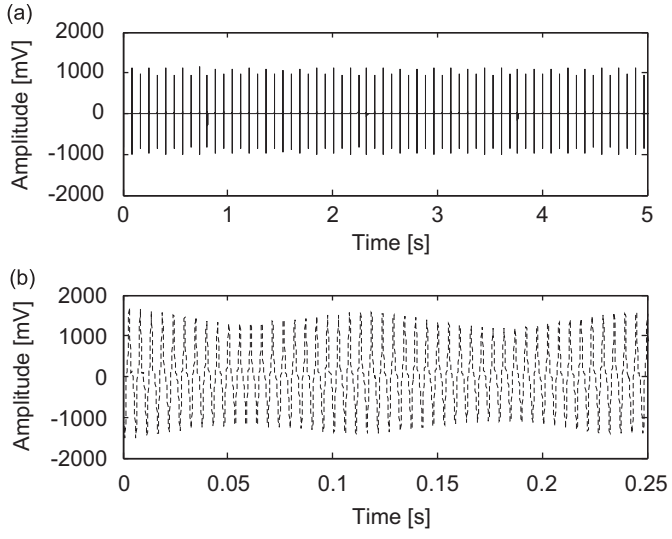

Fig. 2. (a) TDC signal and (b) raw MPU signal.

first cylinder; overlaying the TDC signal with the first cylinder's vibration signal reflects the correct position of the crankshaft referring to the cylinder's TDC position.

By contrast, for laboratory test bed engines the measurement procedure is different. Here a TDC signal is taken from the camshaft or a pressure signal is taken from the cylinder head in order to verify the firing of the first cylinder. However, in terms of the applicability for condition monitoring of large diesel engines, such as marine drives, power generation or emergency generators, the method used for this research is more useful.

4. Experimental evaluation

For internal combustion engines many faults relating to the combustion process can occur. In short there are faults such as leakage or coking of the fuel injection system, valve leakage and serious wearing between the piston and cylinder liner.

The key speed change is expected during the combustion phase of the firing cylinder and hence a fuel leakage in the fuel injection system is simulated. The fault was applied to cylinder B3 and A8 (B-bank three and A-bank eight) of the 16-cylinder engine and to A7 (A-bank seven) of the 20-cylinder engine. The fault was seeded on the 16-cylinder engine mechanically by disconnecting the fuel supply line. The 20-cylinder engine is fully electronically controlled and therefore a fuel fault could be applied to the engine via the electronic control unit (ECU) of the fuel injection system. The lack of fuel in the cylinder will cause a misfire of the cylinder on its combustion stroke and will decrease the operating torque of the crank-connecting link to the crankshaft. The outcome of this is that the torsional power output of the whole engine will shift. Under normal conditions the engine speed will vary from a minimum at TDC to a maximum near the end of the combustion phase and should be periodic and uniform due to almost the same gas pressure for all cylinders. For multi-cylinder engines with a fault, the fault imposed results in a pressure change and also a change in the pattern of the IAS during the combustion phase of all cylinders, because the work done by one cylinder during its combustion phase drives other cylinders in other parts of the cycle [9].

4.1. 16-cylinder engine

To establish a baseline, the raw signal collected from the flywheel encoder has been processed in order to extract the IAS waveform. Fig. 3 shows the measured IAS in the time waveform representation for the engine under healthy conditions (a) and with misfires in cylinder B3 (b) and A8 (c) under 25% load. The TDC trigger

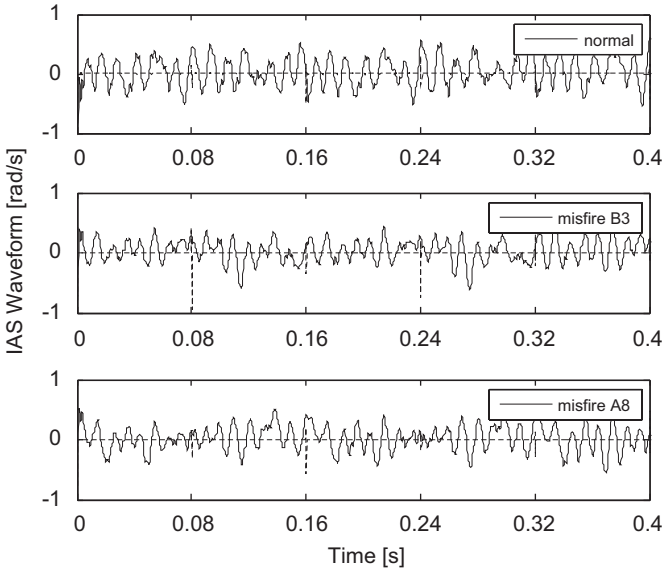

Fig. 3. IAS waveform of the 16-cylinder engine with 25% load and different fault condition.

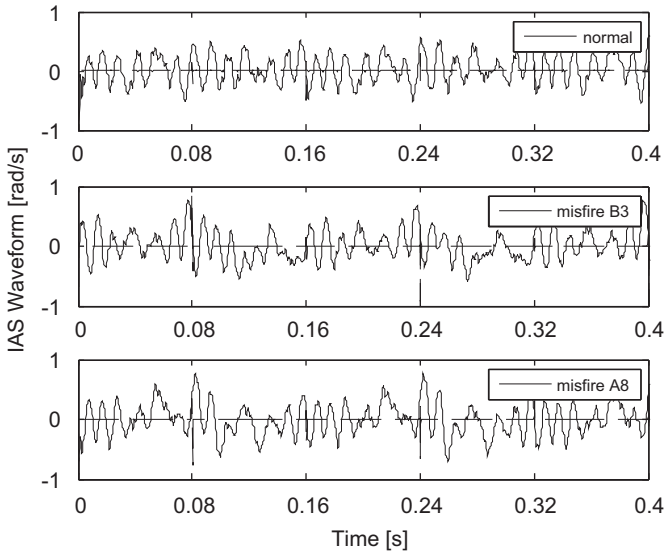

Fig. 4. IAS waveform of the 16-cylinder engine with 50% load and different fault condition.

signal of cylinder A1 has been plotted to identify the corresponding crank angle position. The distinctive speed fluctuation, caused by the torsional vibrations and the small difference between the normal and faulty conditions can be observed in Fig. 3.

Fig. 4 shows the IAS waveforms for the engine under both healthy and faulty conditions at 50% load. The change in the pattern of the IAS waveforms between the healthy and the misfiring (faulty) conditions are definitely significant at 50% load when compared to those at 25%, shown in Fig. 3. However, the crank angle identification related to the faulty cylinder is very imprecise and hence such diagnosis may not be adequate for the remedial action. Engine operation beyond this high load for the faulty engine can cause serious problems and therefore the time-domain presentation may not always be viable to monitor the condition of medium-speed diesel engines.

Fig. 5 shows the raw encoder frequency spectrum. The operating engine speed is 750 rev/min i.e. 12.5 Hz and the number of teeth passing per revolution are 152 (Table 1). Therefore the carrier frequency is 1900 Hz as shown in the zoom window. In Fig. 6 the raw encoder frequency spectra for a healthy and a faulty condition are shown and hardly show any significant difference between the two conditions. However, the spectra of the IAS waveforms shown in the zoom window up to 250 Hz show significant differences between the normal and faulty condition. Multiple-peaks, seen in the IAS spectrum for the faulty engine up to $0.5f_f$ (where $f_f = 100$ Hz), and that there is no prominent peak at the firing frequency and the related higher harmonics, must be indicating some abnormal cylinder firing.

The IAS frequency spectra shown in Fig. 7 for the healthy engine under various loads validates one feature in all of the frequency spectra, i.e. that no new frequency components appear with varying engine loads. Three different loads have been applied to the engine and the main difference is the distinctive amplitude of the spectrum. Fig. 8 illustrates the IAS frequency spectrum up to the firing frequency f_f, for a healthy and two faulty engines. It can clearly be seen that there are a number of frequency peaks with higher amplitudes below $0.5f_f$ for the faulty engines, compared to the healthy one. The behaviour for the two faulty conditions is nearly identical, although the angular crankshaft position of the engine with cylinder B3 misfiring is 45°, whilst it is 360° for the engine with cylinder A8 misfiring (according to Table 1). The analysis using the FFT of the IAS signals is clearly able to distinguish between the faulty and healthy combustion in the diesel engines. It contains information relating to the fault (see Figs. 6–8), but locating the faulty cylinder/cylinders is not possible as it requires phase information related to the engine firing angle. However, for a reliable health monitoring a much better discrimination feature is needed. Hence the polar presentation of the IAS data in two frequency bands was also applied to this case study.

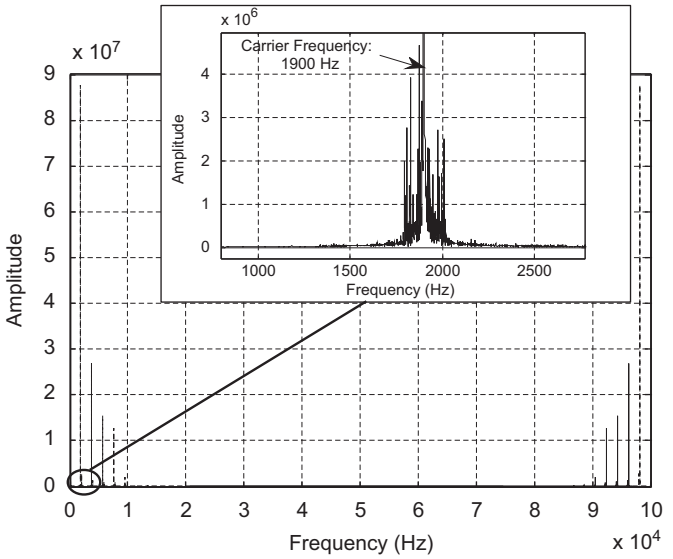

Fig. 5. Spectrum of the speed encoder raw signal for the healthy 16-cylinder engine (zoom view—carrier frequency).

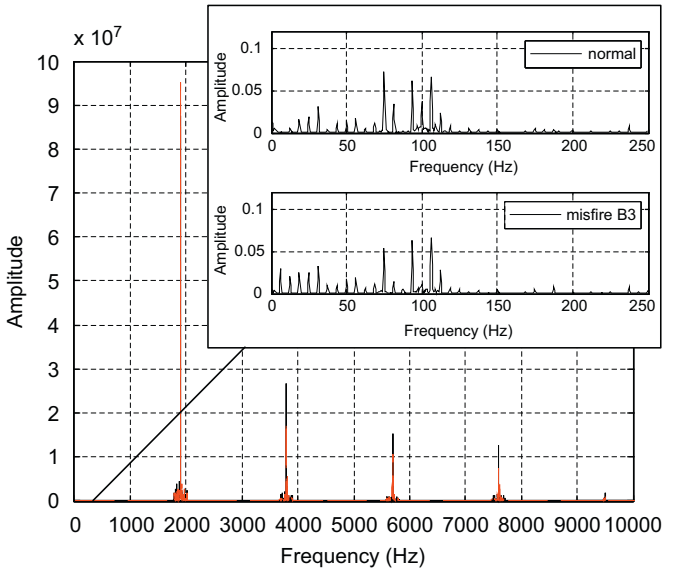

Fig. 6. Spectra of the speed encoder raw signals for a healthy and a faulty 16-cylinder engine (zoom view—spectra of the IAS signals up to 250 Hz).

4.2. Polar presentation method

The IAS waveforms for a healthy and two faulty (misfiring in B3 and A8) conditions were plotted in the proposed polar presentation. The IAS data in two frequency bands as discussed in Section 2.1 has been plotted. One frequency band is related to the frequency content up to the sub-harmonic of the firing frequency ($0.5f_f$) and the other up to the second harmonic of the firing frequency ($2f_f$).

Fig. 9 shows the polar presentation of the IAS signal in the high-frequency range at 50% load. Fig. 9(a) compares the normal (solid line) with the faulty signal (dotted line for A8 misfiring) and it is clear that the lack

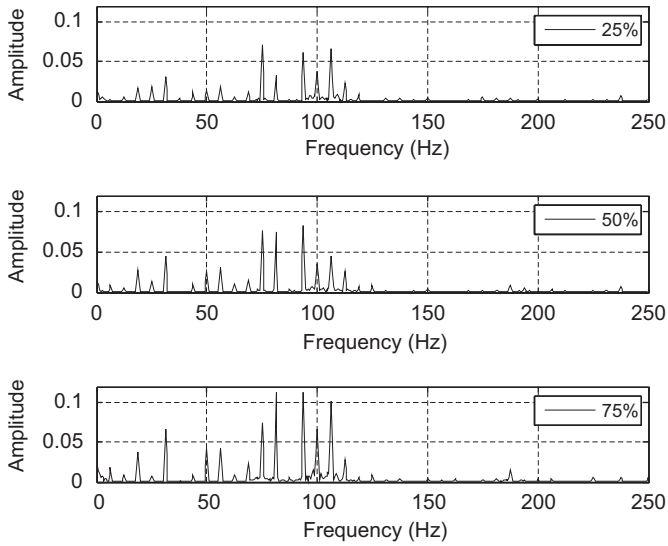

Fig. 7. IAS frequency spectrum—healthy engine condition and different loads.

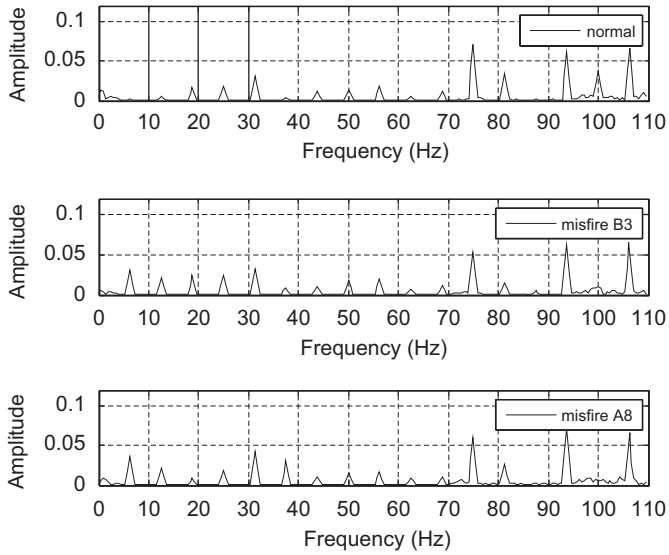

Fig. 8. IAS frequency spectrum—healthy and faulty engine condition under 25% load.

of the combustion of cylinder A8 causes a decrease of the IAS amplitude and a shift of the torsional power output of the whole engine. Fig. 9(b) compares the IAS signals for faulty conditions only—the misfire in B3 (dotted line) and the misfire in A8 (solid line). It can be seen in all of these high-frequency range polar plots, that there is a small axial displacement of the IAS signal, which is caused by the segmentation of the IAS signal into the polar coordinates and the IAS algorithm.

As the varying engine speed of the faulty engine, from a minimum at TDC to a maximum near the end of the combustion phase, is not homogeneous and the pattern of the IAS during the combustion phase of all cylinders is changed, it is difficult to locate the exact angular crankshaft position of the faulty cylinder using the high-frequency plot. However, the low-frequency plot Fig. 10 is fairly smooth compared to the signal of the high-frequency range and gives users clear information about the faulty cylinder. The fact that the work done by one cylinder during its combustion phase drives other cylinders in other parts of the cycle makes the low-frequency method more applicable. Fig. 10(a) compares the healthy condition (solid line) with that of A8

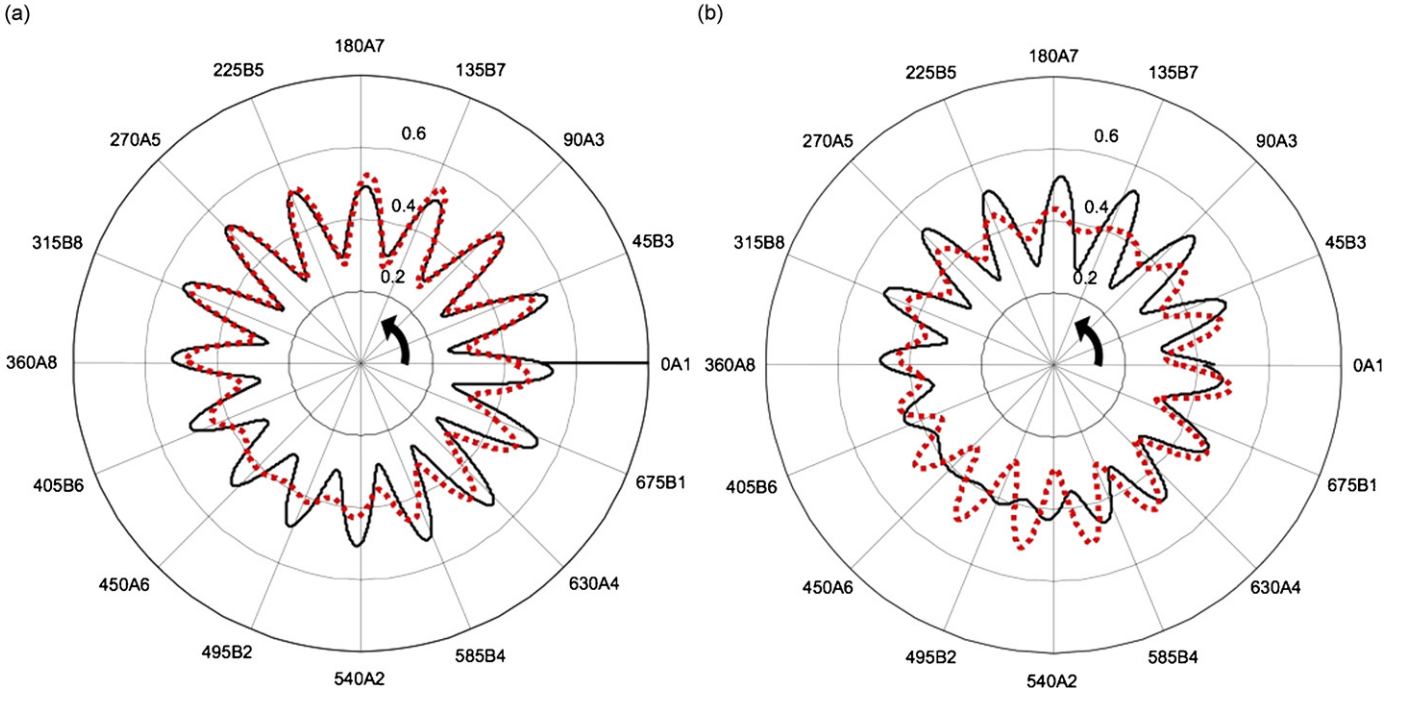

Fig. 9. Polar presentation of the IAS waveforms in high-frequency range for the 16-cylinder engine: (a) healthy (solid line) and A8 misfiring (dotted line) and (b) B3 misfiring (solid line) and A8 misfiring (dotted line).

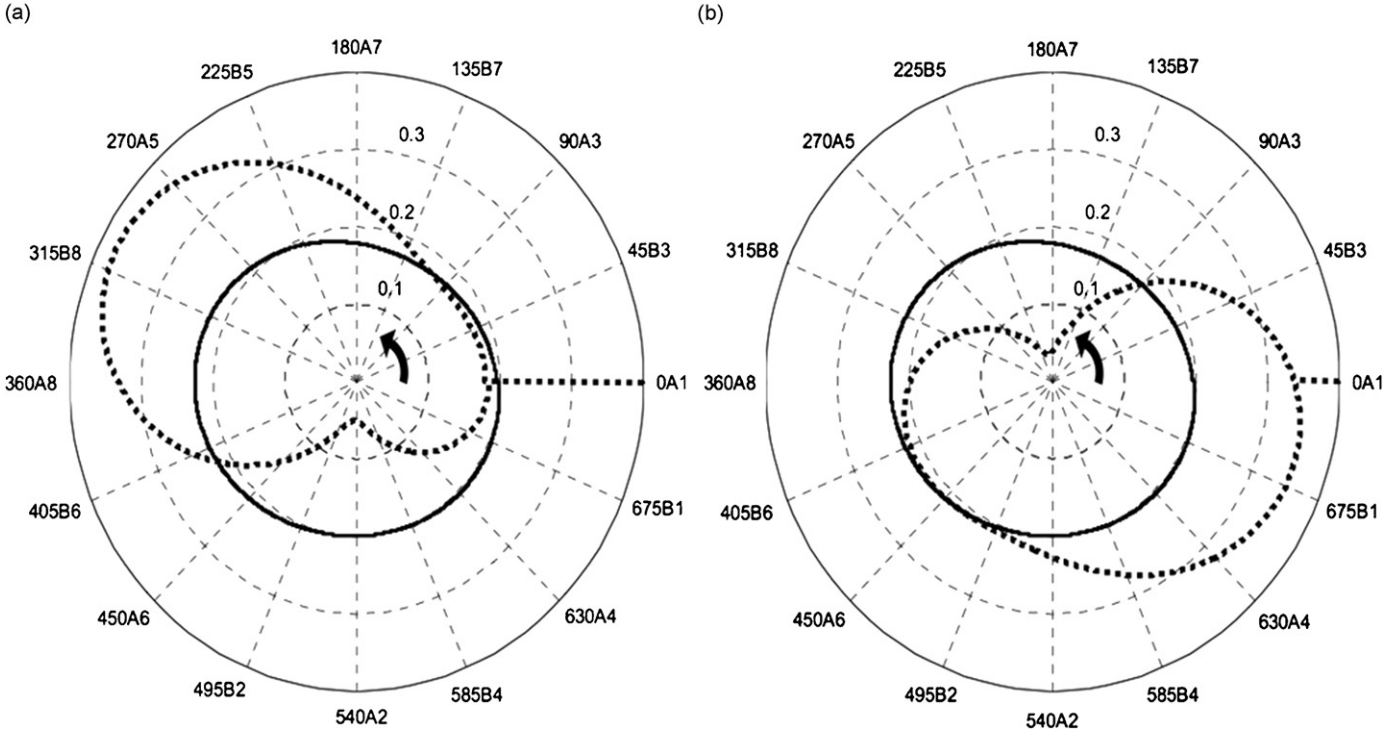

Fig. 10. Polar presentation of the IAS waveforms in low-frequency range for the 16-cylinder engine: (a) healthy (solid line) and A8 misfiring (dotted line) and (b) healthy (solid line) and B3 misfiring (dotted line).

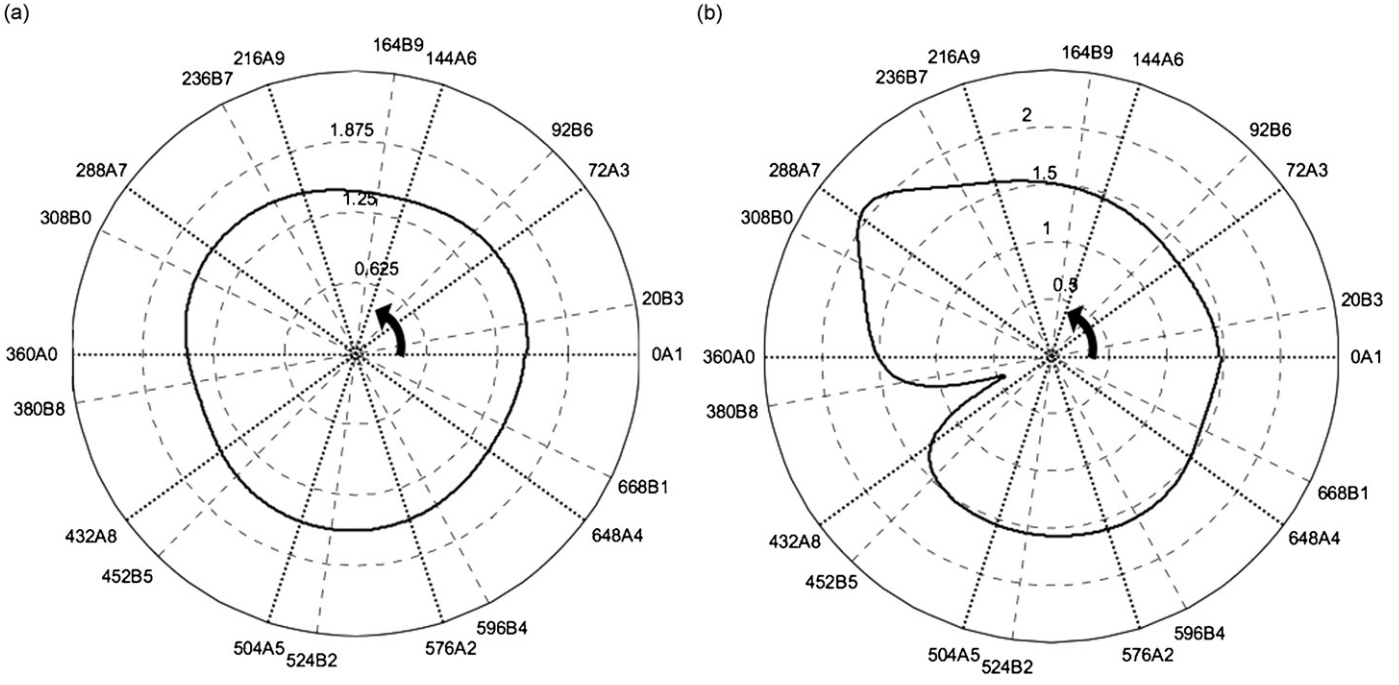

Fig. 11. Polar presentation of the IAS waveforms in the low-frequency range for the 20-cylinder engine: (a) healthy and (b) faulty—A7 misfiring.

misfiring (dotted line) and Fig. 10(b) indicates the differences of the healthy (solid line) and B3 misfiring (dotted line) signal.

4.3. 20-cylinder engine

In this case study it should be noted that the firing angle of the 20 cylinders is not equally spaced. The required technical details are listed in Table 1. Having known that the proposed polar presentation method provides a better method for discriminating between the healthy and faulty conditions, only this method was applied. Here again, data was collected for an engine under healthy conditions and one with a misfiring cylinder (in this case A7). The raw data was processed to construct the IAS signals for the healthy and faulty combustion conditions of the 20-cylinder engine at 50% load. The polar plots in the low-frequency range are shown in Fig. 11. Fig. 11(a) shows the healthy engine condition and Fig. 11(b) plots the faulty engine condition in the low-frequency range. As the angle ϕ_c between consecutive firings is not equal the pattern of the signal is different to that of the 16-cylinder engine. The main reason for this signal distinction is that ϕ_c has two values with the crank angle being only 20° between the faulty cylinder (A7) firing and the healthy cylinder (B10, marked as B0 in Fig. 11) firing. Therefore the expected key speed change of the combustion phase of the next firing cylinder B10 is joined together with the speed increase of cylinder A7. However, Fig. 11 is fairly smooth and referring to the engine firing order (Table 1) it is easy to locate the speed change caused by the misfiring cylinder, as clearly shown in Fig. 11(b).

5. Conclusions

The use of the IAS signal representing the torsional vibration of the crankshaft in diesel engines is perhaps a well recognised tool for engine combustion related diagnosis. However, the fault identification process seems to be more subjective and has only been applied to small diesel engines in the earlier studies reported in the literature. Here also, the IAS time waveform and their FFT analysis were applied to a relatively big engine—a medium-speed 16-cylinder engine. It has been observed that the IAS spectrum was able to distinguish between the healthy and faulty combustion (misfiring) in the 16-cylinder engine but the difference was not prominent enough. However, it is very essential for any reliable condition monitoring to not only identify the presence of faults but also their locations. Hence a novel approach for presenting the IAS data using polar coordinates relating to both the cylinder firing order angles and the amplitude of torsional vibration has been proposed. The proposed method has been applied to the two medium-speed diesel engines (16 cylinders and 20 cylinders) with healthy and faulty (misfiring) combustion conditions. The proposed method successfully identifies both the faults and the particular faulty cylinder. The results of the earlier approach, the FFT analysis of the IAS signal, have also been compared in the present study. In fact, the successful application in the 20-cylinder engine by the proposed method itself highlights the ruggedness of the proposed polar presentation method. Although the cylinder firing angles were not equally spaced the method was still able to identify both the fault and the faulty cylinder. Subsequently, it is intended to test the proposed polar method with smaller combustion faults such as fuel injection faults, cam valve malfunctions, etc. which will be reported separately.

References

[1] F. Gu, P.J. Jacob, A.D. Ball, Non-parametric models in the monitoring of engine performance and condition—part 2: non-intrusive estimation of diesel engine cylinder pressure and its use in fault detection, *Proceedings of the Institution of Mechanical Engineers, Part D—Journal of Automobile Engineering* 213 (1999) 73–81.

[2] M. Feldman, S. Seibold, Damage diagnosis of rotor: application of Hilbert transform and multihypothesis testing, *Journal of Vibration and Control* 5 (1999) 421–442.

[3] P.J. Sweeney, R.B. Randall, Gear transmission error measurement using phase demodulation, *Proceedings of the Institution of Mechanical Engineers Part C—Journal of Mechanical Engineering Science* 210 (1996) 201–213.

[4] J. Yang, L. Pu, Z. Wang, Y. Zhou, X. Yan, Fault detection in a diesel engine by analysing the instantaneous angular speed, *Mechanical Systems and Signal Processing* 15 (3) (2001) 549–564 (16).

[5] G.F. Mauer, Modelling and experimental validation of torsional crankshaft speed fluctuation: a model for dynamics of IC engine, SAE Technical Paper No. 940630, 1994.

[6] G.F. Mauer, On-line cylinder fault diagnosis for internal combustion engines, *IEEE Transactions on Industrial Electronics* 37 (3) (1990) 221–226.
[7] G. Rizzoni, Diagnosis of individual cylinder misfires by signature analysis of crankshaft speed fluctuations, *Presented at SAE International Congress and Exposition*, SAE Paper No. 890884, Detroit, MI, February 27–March 3, 1989, pp. 1–10.
[8] I.E. Margaronis, The torsional vibrations of marine diesel engines under fault operation of its cylinders, *Forschung im Ingenieurwesen* 56 (1–2) (1992) 13–25.
[9] P. Charles, D. J. Moore, F. Gu, A.D. Ball, An investigation of the flywheel speed fluctuation of large diesel engine applications, *Second World Congress on Engineering Asset Management and Fourth International Conference on Condition Monitoring* (*WCEAM-CM 2007*), Harrogate, UK, 11–14 June 2007.
[10] D. Vakman, New high precision frequency measurement, *Measurement Science and Technology* 11 (2000) 1493–1497.
[11] F. Gu, I. Yesilyurt, Y. Li, G. Harris, A. Ball, An investigation of the effects of measurement noise in the use of instantaneous angular speed for machine diagnosis, *Mechanical Systems and Signal Processing* 20 (6) (2006) 1444–1460.